

Fatigue studies of high-palladium dental casting alloys: Part I. Fatigue limits and fracture characteristics*

D. LI¹, W. A. BRANTLEY[†], J. C. MITCHELL², G. S. DAEHN³, P. MONAGHAN¹, E. PAPAZOGLU⁴

¹*Section of Restorative Dentistry, Prosthodontics and Endodontics,*

²*Department of Geological Sciences, and* ³*Department of Materials Science and Engineering, Section of Restorative Dentistry, Prosthodontics and Endodontics, College of Dentistry, The Ohio State University, Columbus, OH, USA*

⁴*Private practice, Athens, Greece*

E-mail: brantley.1@osu.edu

The fatigue limits and fracture characteristics for a Pd–Cu–Ga alloy and a Pd–Ga alloy were studied. The alloys were cast into tensile test bars with gauge diameter of 3 mm and gauge length of 15 mm, and the surfaces of the castings were neither air-abraded nor polished after removal from the investment. Specimens were prepared from all-new metal (not previously melted), a combination of 50% new metal and 50% old metal (previously melted one time) and 100% old metal. The cast bars were subjected to heat treatment simulating the complete firing cycles for dental porcelain, and fatigued in air at room temperature under uniaxial tension-compression stress at 10 Hz and a ratio of tensile stress amplitude to compressive stress amplitude (*R*-ratio) of -1 . The alloy microstructures and fracture surfaces were examined with a scanning electron microscope (SEM). Results showed that the fatigue limits at 2×10^6 cycles of the Pd–Cu–Ga and Pd–Ga alloys were approximately 0.20 and 0.15 of their 0.1% yield strength (YS) in tension, respectively. The fatigue resistance for specimens from both alloys containing 50% old metal and 50% new metal was comparable to that of specimens containing all-new metal, although this decreased dramatically for Pd–Cu–Ga alloy specimens containing all-old metal. The fatigue resistance of the Pd–Cu–Ga alloy subjected to heat treatment simulating the porcelain firing cycles was not adversely affected by remnants of the original as-cast dendritic microstructure that remained in the relatively large test specimens. A longer heat treatment than recommended by the manufacturer for the porcelain firing cycles is needed to completely eliminate the as-cast dendritic structure in these specimens. The Pd–Cu–Ga alloy exhibited superior fatigue resistance to the Pd–Ga alloy, which has an equiaxed-grain microstructure and lower yield strength.

© 2002 Kluwer Academic Publishers

1. Introduction

Since their introduction in the early 1980s as economical alternatives to traditional gold-based alloys, the high-palladium dental casting alloys, which contain approximately 75 wt % or more palladium and are based upon Pd–Cu–Ga or Pd–Ga systems, have been extensively used for metal-ceramic restorations [1] and implant-supported prostheses [2]. While current use has been diminished by the price volatility of palladium, these alloys have been popular because of their excellent mechanical properties [3, 4], good porcelain adherence [5–7] and absence of porcelain discoloration [8].

Fatigue is a mode of fracture whereby a metallic

structure eventually fails after being repeatedly subjected to loads substantially below the yield strength, where one application of such a load apparently is not detrimental to the component [9]. However, when subjected to cyclic stresses of sufficient magnitude, almost any manufactured metallic component will fail by fatigue [10]. The fatigue behavior of metals and the methodology for fatigue testing are discussed at length in textbooks on the mechanical behavior of materials [11, 12]. Although clinical evidence indicates that the majority of fractures that occur in dental materials are generally not related to an episode of acute overload, but instead result from fatigue failure [10], little research on the fatigue behavior

*A portion of this study was presented at the 30th annual meeting of the American Association for Dental Research, Chicago, IL, March 2001.

[†]Author to whom all correspondence should be addressed: Section of Restorative Dentistry, Prosthodontics and Endodontics, College of Dentistry, The Ohio State University, PO Box 182357, Columbus, OH, USA 43218-2357.

TABLE I Compositions (wt %) of Spartan Plus and Protocol high-palladium alloys

Alloy	Pd	Ga	Cu	In	Au	Ag	Ru	Ir	Other
Spartan Plus	78.8	9.0	10	0	2	0	—	< 1.0	Ge < 1.0, Li < 1.0
Protocol	75.2	6.0	—	6.0	6.0	6.5	< 1.0	—	Li < 1.0

From the product information literature (Williams/Ivoclar, Amherst, NY).

of dental casting alloys has been reported. In our previous presentation [13], the fatigue fracture characteristics of two Pa–Cu–Ga alloys were described. The purpose of the present study was to investigate in detail the fatigue limit and the fracture characteristics for a different Pd–Cu–Ga alloy and a representative Pd–Ga alloy.

2. Materials and methods

Two high-palladium alloys, Spartan Plus (Pd–Cu–Ga) and Protocol (Pd–Ga), were selected for this study. Both alloys are manufactured by the Williams Division of Ivoclar North America, Amherst, NY. In the as-cast condition, Spartan Plus exhibits a dendritic microstructure [14], while Protocol has an equiaxed-grain microstructure [1, 15]. The alloy compositions (wt %) given by the manufacturer are listed in Table I.

The alloys were cast into tensile test bars having a gauge diameter of 3 mm and gauge length of 15 mm, which satisfy the dimensional requirements in ADA Specification Nos. 5 [16] and 38 [17]. Polystyrene plastic patterns (Salco, Romeoville, IL, USA) [18] conforming to these dimensions were sprued and invested in fine-grained, carbon-free, phosphate-bonded investment (Cera-Fina, Whip-Mix, Louisville, KY, USA). Investment manipulation and burnout procedures followed the recommendations of the manufacturer. Two specimens of each alloy were cast for each test condition (to be described later), and all castings were bench-cooled to room temperature, which is recommended dental laboratory practice for these alloys. After removal from the investment, the sprues were cut from the specimen with a carborundum separating disk, and any visible nodules were carefully eliminated. The specimens used in the fatigue testing had the as-cast surface condition, and were not subsequently air-abraded or polished. Three groups of specimens were fabricated for testing. Group I specimens were prepared from metal that had not previously been melted (“new metal”). Group II specimens (50/50%) were prepared from 50% “new metal” and 50% “old metal” that had been previously melted one time. Group III specimens were prepared from 100% “old metal” (previously melted one time).

Prior to the preparation of the Groups II and III specimens, the previously melted metal was carefully polished, using silicon carbide paper to completely remove the surface oxidation layer, and then ultrasonically cleaned in acetone before casting.

Heat treatment simulating the complete porcelain-firing cycles was carried out in a conventional dental porcelain furnace (Ultra-Mat CDF, 3M Unitek, Monrovia, CA, USA). The initial oxidation treatment followed the instructions of the alloy manufacturer, and the subsequent firing cycles followed the recommendations [5] for VMK porcelain (Vident, Baldwin Park, CA, USA). Important mechanical properties of both alloys in the simulated porcelain-firing heat-treated condition are given in Table II, where both published research data [3, 4] and values reported by the manufacturer are provided. Calculations of the appropriate loads to produce the desired stress amplitudes for the fatigue experiments were based upon published values [3, 4] of the yield strengths (YS) for 0.1% permanent tensile strain ($\sigma_{0.1}$) of these two alloys, rather than the values reported by the manufacturers. (Other than the elastic modulus, which is the most difficult property to measure accurately with these small castings, the measured [3, 4] mechanical properties in Table II and those reported by the manufacturer generally agree within 10% or less.) Starting stress amplitudes for the fatigue experiments were based upon pilot experiments performed on specimens prepared from scrap metal that had been previously melted more than one time. This resulted in the use of considerably fewer specimens of each alloy to determine the approximate fatigue limit, compared to that needed with conventional staircase methods [11, 12].

The fatigue tests were carried out in air at room temperature using a uniaxial sinusoidal tension–compression loading regimen with a servohydraulic mechanical testing machine (Model 1322, Instron Corp., Canton, MA, USA). The stress ratio (R) between the tensile and compressive stress amplitudes and the frequency were -1 and 10 Hz, respectively. Two replicate specimens were tested at each stress, and the stress at which fracture did not occur after 2×10^6 cycles was designated as the fatigue limit. This number of cycles was selected to provide clinically relevant

TABLE II Mechanical properties of Spartan Plus and Protocol high-palladium alloys

Alloy	Yield strength $\sigma_{0.1}$ (MPa)	Yield strength $\sigma_{0.2}$ (MPa)	Tensile strength UTS (MPa)	Elongation (%)	Elastic modulus E (GPa)
Spartan Plus*	700	725	1002	24	141
Spartan Plus†	634	795	—	20	97
Protocol*	534	552	770	35	123
Protocol†	474	500	—	34	103

*From Papazoglou *et al.* [3] and [4]. Data for simulated porcelain-fired specimens.

†From the product information literature (Williams/Ivoclar). The data are for the simulated porcelain-fired heat-treated condition.

TABLE III Number of cycles to failure for Group I specimens of Spartan Plus and Protocol alloys (all-new metal) tested at different stress amplitudes (loads)

Specimen number	Alloy	Stress (load N)	Fatigue cycles
1	Spartan Plus	0.25 $\sigma_{0.1}$ (1237)	68 973
2		0.25 $\sigma_{0.1}$ (1237)	79 687
3		0.20 $\sigma_{0.1}$ (943)	1 908 825
4	Protocol	0.20 $\sigma_{0.1}$ (943)	1 719 015
5		0.25 $\sigma_{0.1}$ (943)	675 250
6		0.25 $\sigma_{0.1}$ (943)	439 822
7		0.20 $\sigma_{0.1}$ (752)	729 935
8		0.20 $\sigma_{0.1}$ (752)	1 117 735
9		0.15 $\sigma_{0.1}$ (564)	> 2 000 000
10		0.15 $\sigma_{0.1}$ (564)	> 2 000 000

information [10], without having a prolonged period of testing. After ultrasonic cleaning in ethanol, the fracture surfaces were examined with a scanning electron microscope (SEM) (JSM-820, JEOL Ltd., Tokyo, Japan) over a range of magnifications. After the fatigue tests, microstructural observations were carried out with the same SEM on flat samples that were sectioned from the fractured bars, using a slow-speed water-cooled diamond saw, and then mounted in transparent metallographic epoxy resin (Leco Corp., St. Joseph, MI, USA). After grinding with 320, 400, and 600 grit silicon carbide papers and polishing with a series of gamma-alumina slurries ending with 0.05 μm particles, the samples were etched in aqua regia solutions [15], using appropriate times to obtain the optimum microstructures.

3. Results

3.1. Fatigue limits for specimens prepared from all-new metal

Table III lists the number of cycles to failure for the Group I specimens (all-new metal) of the Spartan Plus and Protocol alloys for different stress amplitudes. The fatigue limits of Spartan Plus and Protocol were approximately 0.20 and 0.15 of the 0.1% YS in tension, respectively. At the same stress amplitude (943 N), Table III shows that Spartan Plus, which has an approximately 30% higher 0.1% YS than Protocol (Table II), required many more cycles for failure.

3.2. Effects of old metal on fatigue limits

At the stress amplitude equal to the fatigue limit for all-new metal specimens in Table III, both of the Group II specimens for 50/50% Protocol survived 2×10^6 cycles (Table IV). Hence, it would be expected that castings prepared from 50% old metal (melted one time) and 50% new metal of Protocol would have similar fatigue performance to castings prepared from all-new metal of this alloy. For 50/50% Spartan Plus, one of the two Group II specimens survived 2×10^6 cycles, and the other specimen failed after 1 371 835 cycles. Since the stress amplitude-dependence of the fatigue limit for Spartan Plus in Tables III and IV is quite pronounced, castings prepared from this alloy with the common dental laboratory procedure of 50% old metal and 50% new

TABLE IV Number of cycles to failure for 50/50% Protocol and Spartan Plus alloys (Group II specimens) and all-old metal Spartan Plus alloy (Group III specimens) tested at different stress amplitudes (loads)

Specimen number	Alloy	Stress (load, N)	Fatigue cycles
1	50/50%	0.15 $\sigma_{0.1}$ (564)	> 2 000 000
2	Protocol	0.15 $\sigma_{0.1}$ (564)	> 2 000 000
3	50/50%	0.20 $\sigma_{0.1}$ (943)	> 2 000 000
4	Spartan Plus	0.20 $\sigma_{0.1}$ (943)	1 371 835
5	All-old metal	0.20 $\sigma_{0.1}$ (943)	357 027
6	Spartan Plus	0.20 $\sigma_{0.1}$ (943)	362 594
7		0.15 $\sigma_{0.1}$ (742)	785 865
8		0.15 $\sigma_{0.1}$ (742)	> 2 000 000
9		0.10 $\sigma_{0.1}$ (495)	> 2 000 000
10		0.10 $\sigma_{0.1}$ (495)	> 2 000 000

metal [19] should also have comparable fatigue resistance to castings prepared from all-new metal.

The number of fatigue cycles to failure for the all-old metal Spartan Plus specimens in Group III, tested at different stress amplitudes, is also shown in Table IV. It was found for the Group III specimens that the fatigue limit of Spartan Plus decreased to approximately 0.10 of the 0.1% YS, that is, when the proportion of old metal increased from 50% to 100% (all-old metal), the fatigue resistance of this alloy decreased considerably.

3.3. Characteristics of fatigue fracture surfaces

SEM observations revealed that the fatigue fracture surfaces of specimens for both alloys tested in this study had characteristic fine striations [11, 12], approximately 0.25–0.5 μm in width, as shown in Figs 1 and 2. The fracture surface topography was particularly complex for the Spartan Plus alloy, where quasi-cleavage fracture was also observed in some areas, as shown in Fig. 3(a) and (b). These figures also indicate that ridges, of coarser scale than the fatigue striations, existed on the fracture surfaces of both alloys.

For the fractured specimens, it was often impossible to unambiguously identify the sites of fatigue fracture

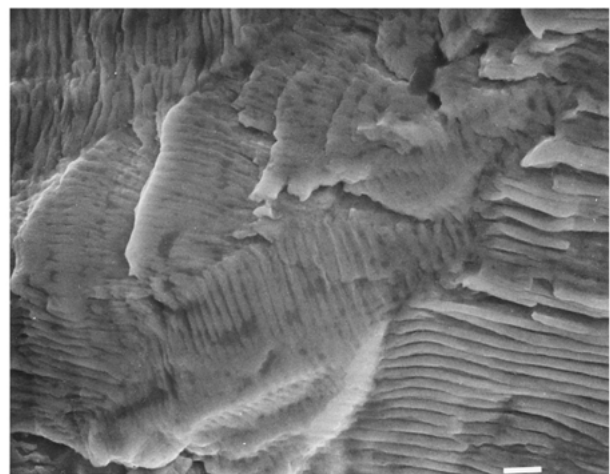


Figure 1 Secondary electron image of the fatigue fracture surface for Spartan Plus (all-new metal, 1 908 825 cycles at 0.20 $\sigma_{0.1}$), showing several orientations of fine-scale striations. (Scale bar length = 1 μm .)

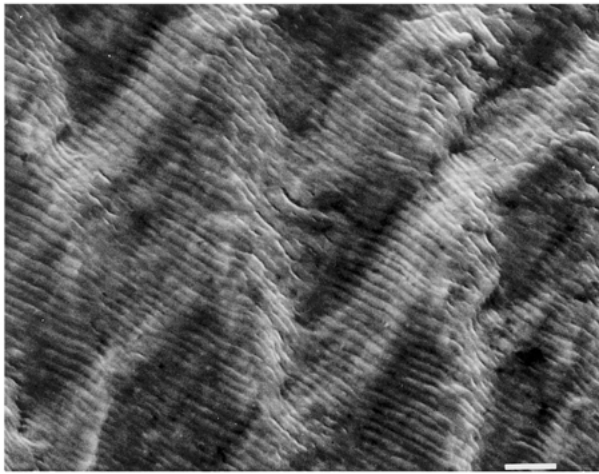
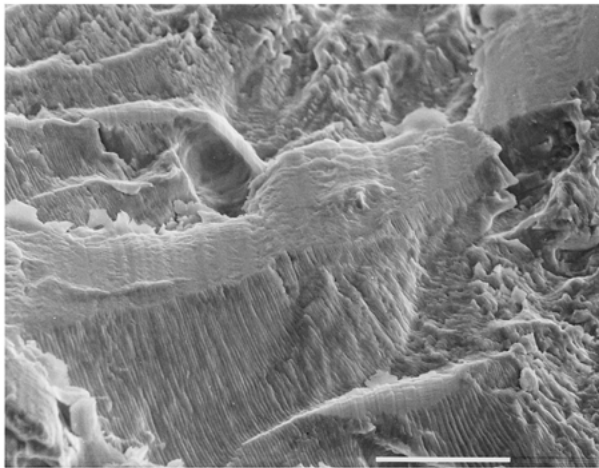
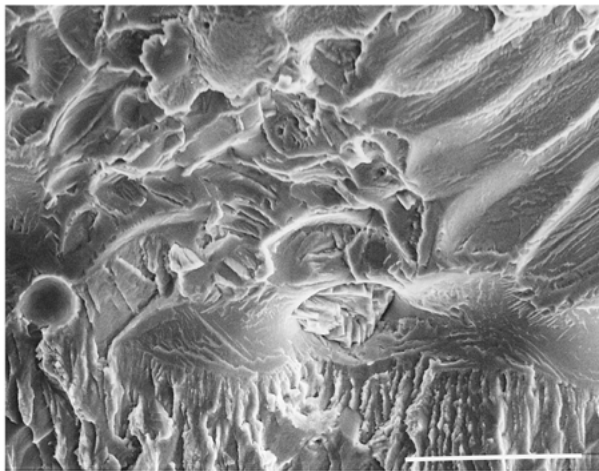


Figure 2 Secondary electron image of the fatigue fracture surface for Protocol (all-new metal, 1 117 735 cycles at $0.20 \sigma_{0.1}$), showing fine-scale striations superimposed on ridges in the microstructure which subsequently formed during the fatigue fracture process. (Scale bar length = $1 \mu\text{m}$.)

initiation. The fatigue crack either initiated at the specimen surface (Fig. 4) or at some microstructural defect within the specimen. In the latter case, for some specimens no obvious fracture initiation site could be



(a)



(b)

Figure 3 Secondary electron images showing the complex fatigue fracture surface topography for Spartan Plus, where regions of quasi-cleavage can be observed along with fine-scale striations. (a) All-new metal, 1 719 015 cycles at $0.20 \sigma_{0.1}$. (Scale bar length = $10 \mu\text{m}$.) (b) All-new metal, 68 973 cycles at $0.25 \sigma_{0.1}$. (Scale bar length = $10 \mu\text{m}$.)

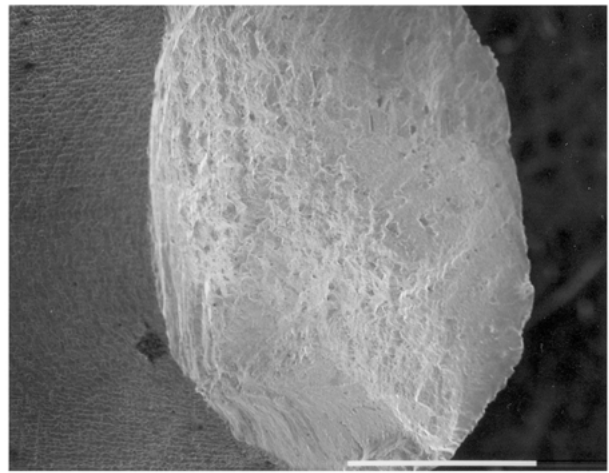


Figure 4 Low-magnification secondary electron image of the fatigue fracture surface for Spartan Plus (all-old metal, 362 594 cycles at $0.20 \sigma_{0.1}$). The initiation site is located at the lower left region of the fracture surface. (Scale bar length = 1mm .)

identified (Fig. 5), while for other specimens there were many possible candidates (Fig. 6).

3.4. Microstructural observations on polished and etched cross-sections

Minimal porosity was observed for the Spartan Plus and Protocol specimens, consistent with previous observations of the microstructures of these relatively large castings [3, 4].

For Spartan Plus, residual dendritic structures were observed for the fractured specimens, both at the external surface (Fig. 4) and within the interior (Fig. 6), indicating that the porcelain-firing heat treatment did not completely eliminate the as-cast dendritic structures. However, this does occur [15] with smaller castings of the Spartan alloy (Williams/Ivoclar), whose composition is nearly identical. Fig. 7 shows that the typical bulk microstructure of the present Spartan Plus specimens after the simulated porcelain-firing heat treatment consisted of the palladium solid solution (the gray background area), small precipitates tentatively identi-

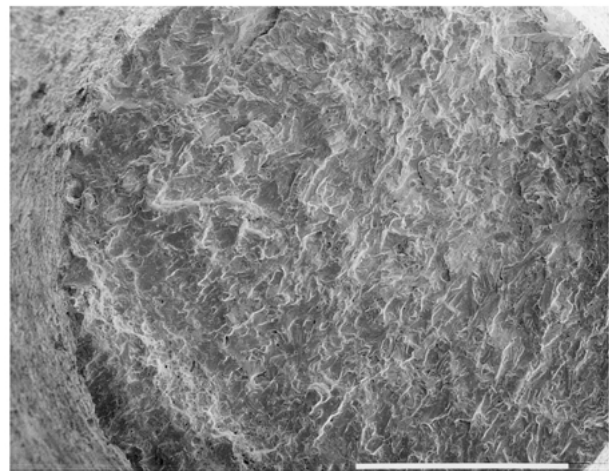


Figure 5 Low-magnification secondary electron image of the fatigue fracture surface for Protocol (all-new metal, 1 117 735 cycles at $0.20 \sigma_{0.1}$), showing no obvious initiation site. (Scale bar length = 1mm .)

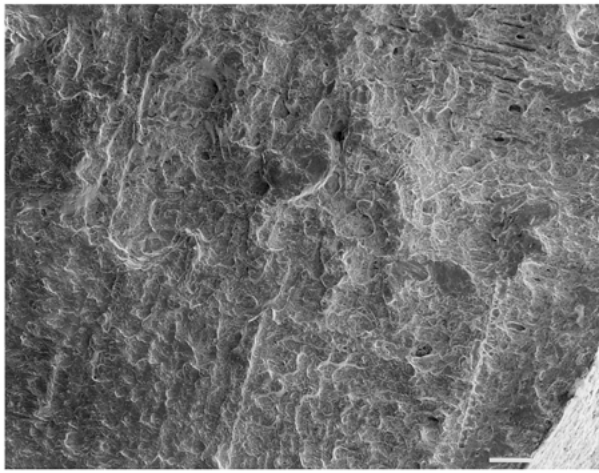


Figure 6 Low-magnification secondary electron image of the fatigue fracture surface for Spartan Plus (all-new metal, 1908825 cycles at $0.20\sigma_{0.1}$), showing many possible initiation sites. The residual dendritic structure of the heat-treated alloy is evident at this magnification. (Scale bar length = 100 μm .)

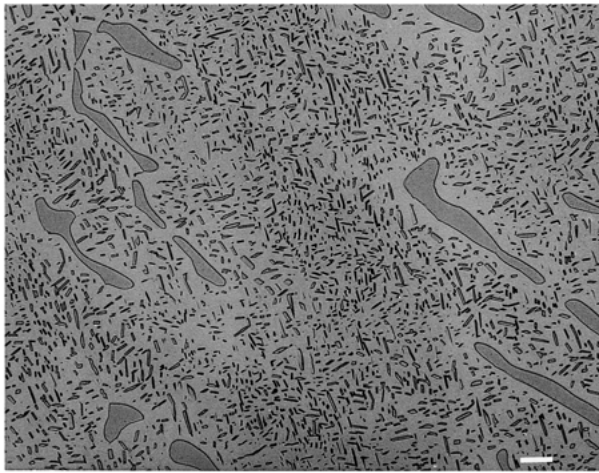
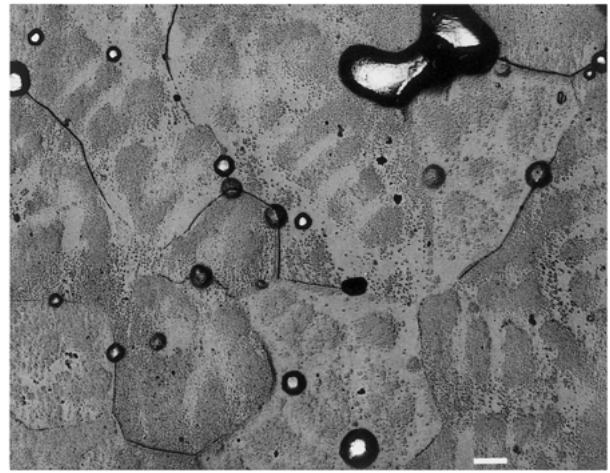


Figure 7 Secondary electron image showing the typical residual dendritic structure of a polished and etched section of a Spartan Plus fatigue test specimen that was subjected to heat treatment simulating the porcelain-firing cycles. (Scale bar length = 10 μm .)

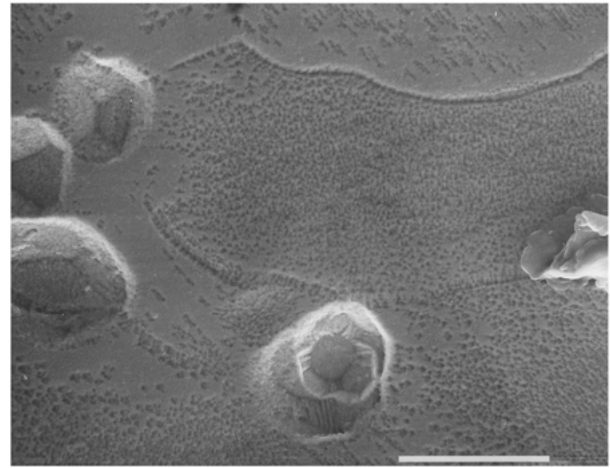
fied as Pd_2Ga and perhaps other Pd–Ga phases from previous studies [3, 20], and remnants of the dendritic structure (the elongated features).

For Protocol, the grain size ranging from approximately 20 μm to over 40 μm in the fatigue test specimens, shown in Fig. 8(a), was substantially larger than the grain size of approximately 10–25 μm previously reported [1, 15] for smaller castings of this alloy that simulated the coping for a maxillary central incisor restoration. Relatively heavy etching revealed bands within the grains, suggesting that vestiges of a residual dendritic structure remained after heat treatment of this alloy. At higher magnification, shown in Fig. 8(b), each of the dark bands in Fig. 8(a) was resolved into a very large number of submicron pits where localized attack by the etchant led to loss of submicron precipitates. In addition, the larger pits of approximately 10 μm dimensions and greater in Fig. 8(a) are clearly shown in Fig. 8(b) to be sites that were formerly occupied by precipitates lost during etching.

For both Spartan Plus and Protocol, no general differ-



(a)



(b)

Figure 8 Backscattered electron images of the typical microstructure for a polished and etched section of a Protocol fatigue test specimen that was subjected to heat treatment simulating the porcelain-firing cycles. (a) Lower-magnification micrograph showing equiaxed grains with internal bands and pits corresponding to former sites of precipitates. (Scale bar length = 10 μm .) (b) Higher-magnification micrograph showing that the dark bands in (a) contain very large numbers of submicron pits due to attack by the etchant. The polyhedral geometry of the sides of the large pits indicates that these sites were formerly occupied by precipitates. (Scale bar length = 10 μm .)

ences in the microstructures were observed for the all-new metal specimens or for the specimens that contained 50% or 100% old metal. However, the possibility that the latter two groups of specimens contained small additional amounts of porosity or other casting defects, compared to the all-new metal specimens, cannot be excluded and requires further investigation.

4. Discussion

4.1. Interaction between fatigue stress and alloy microstructure

Although microstructural porosity in dental alloy castings is decreased with the proper use of the standard centrifugal casting technique, casting porosity cannot be completely eliminated and is sensitive to a variety of laboratory manipulations [21]. Casting defects, especially those at or near the surfaces, are extremely prone to become fatigue crack initiation sites in alloys [22–24]. It was generally not possible in this study to identify

unambiguously the fatigue crack initiation sites with the SEM, either at the surface or within the bulk specimen. Consequently, no particular type of microstructural feature (defect or constituent) always acted as a preferential site for fatigue crack initiation in Spartan Plus and Protocol. This appears to be a favorable property for the two high-palladium alloys.

During the fatigue crack propagation process, the interaction between the cyclic stress and the alloy microstructure is complicated. As shown in Fig. 3(a) and 3(b) for Spartan Plus, in addition to the fine striations for fatigue fracture, more rapid brittle fracture of secondary phase particles and quasi-cleavage also occurred in this complex microstructure. The fine striations, characteristic of fatigue fracture, result from the interaction of the advancing fatigue crack with the material under cyclic stresses [11,12]. Because the ridges in Fig. 3(a) and (b) are coarser than the lamellar eutectic constituents typically observed in the interdendritic regions of as-cast Spartan Plus [20], it is assumed that they were created by the advancing fatigue crack front, perhaps as a result of interactions with the residual interdendritic structure or with the Pd₂Ga phase or other Pd–Ga phases.

The fine striations in Protocol were superimposed on ridges (Fig. 2), which were not previously observed with the SEM on fracture surfaces of similar heat-treated Protocol specimens that were loaded to failure in tension [4]. Consequently, it is assumed that these ridges were created during the fatigue fracture process, perhaps by the interactions of stress waves. Careful examination of Fig. 2 suggests that the ridges were formed after the striations, since the latter are sometimes not continuous across adjacent ridges. Moreover, the ridges are narrower than the bands within the etched grains of this alloy, shown in Fig. 8(a). Further research on the origin of these microstructural features in heat-treated Protocol is needed. Moreover, examination of fractured fatigue test specimens, and polished and etched cross-sections of specimens, for both Pd–Cu–Ga and Pd–Ga dental alloys that have equiaxed-grain as-cast microstructures, would show whether the microstructural observations in the present study for Protocol are unique or are general occurrences for all high-palladium alloys of this type. A complementary transmission electron microscopy study [25] has revealed that the microplastic deformation modes of Spartan Plus and Protocol during fatigue loading are considerably different.

4.2. Fatigue limit

The fatigue limit is directly related to the resistance of the material to both fatigue crack initiation and crack propagation, which can vary with both the alloy composition and microstructure. In contrast to the present investigation, it was previously found, in a preliminary study of two other Pd–Cu–Ga alloys in the as-cast condition [13], that the alloy with the equiaxed-grain microstructure (Freedom Plus, J. F. Jelenko & Company, Armonk, NY, USA) was more fatigue-resistant than the alloy with the dendritic microstructure (Option, Degussa-Ney, Bloomfield, CT, USA). However, this earlier investigation employed a cantilever bending

technique, rather than uniaxial tension–compression loading.

In the present study, after heat treatment simulating the porcelain firing cycles, the Spartan Plus alloy, which contained remnants of the original as-cast dendritic microstructure, nonetheless had a higher ratio of fatigue limit to yield strength [3] than did Protocol [4]. The latter alloy has an equiaxed-grain microstructure in the as-cast condition [14,15], but relatively heavy etching of the microstructure (Fig. 8) also suggested that there may be a residual dendritic structure within the grains, even after the simulated porcelain-firing heat treatment. While the present results show that the fatigue limit for heat-treated Spartan Plus is not drastically affected by the residual dendritic structure, this microstructure evidently has a substantial role for the fatigue fracture surface morphology, as suggested by Fig. 1 and Fig. 3(a) and (b). The higher fatigue limit of Spartan Plus, compared to Protocol (Tables III and IV), is attributed to the greater yield strength of the former alloy (Table II) and to fundamentally different mechanisms for microplastic deformation during fatigue loading [25]. It should be emphasized that careful clinical investigations comparing the performance of these two alloys would be required to determine whether the lower fatigue limit of Protocol compared to Spartan Plus is of practical concern.

The fatigue limit can be affected by many different testing variables, such as the type of loading (uniaxial, bending or torsional), loading pattern (cyclic loading at constant or variable amplitude), loading magnitude (different *R* values resulting in different fatigue limits), and the designated number of cycles to be tested [11,12]. Therefore, the values of fatigue limit determined in a given study are frequently not applicable for comparison to the fatigue properties for the same alloy under different testing conditions. The present cyclic uniaxial tension-compression loading is a very severe fatigue-testing mode, because the whole cross-section of the specimen undergoes uniform cyclic stresses. Although Spartan Plus and Protocol have a comparatively low ratio of fatigue limit to yield strength (about 0.15 – 0.20), this does not mean that these two high-palladium alloys are not relatively fatigue-resistant, compared to other types of dental casting alloys where information about fatigue properties is not presently available. While it is tempting in the present study to ascribe the low ratio of fatigue limit to yield strength to casting or microstructural defects in the high-palladium alloy specimens, further observations are necessary at both the SEM and TEM levels to fully identify the major factors affecting the fatigue properties of these alloys. At present, there are no fatigue testing specifications for dental materials, and it is difficult to obtain meaningful comparisons of the fatigue properties of dental alloys from different laboratories or manufacturers. The development of a standardized fatigue testing protocol for dental casting alloys is an important area for future research.

4.3. Difference in fatigue behavior for all-old metal

An investigation of the effects of recasting high-palladium alloys on porcelain adherence [7] demon-

strated that recasting both Spartan Plus and Protocol without adding any new metal caused a dramatic decrease in porcelain adherence. From the present results, both Spartan Plus and Protocol test specimens containing 50% old metal (Group II) have comparable fatigue resistance to test specimens fabricated from entirely new metal (Group I), while Spartan Plus specimens consisting entirely of once-melted metal (Group III) exhibited dramatically deteriorated fatigue resistance. Although no distinct microstructural differences were observed with the SEM for the all-old, all-new and 50% new-metal/50% old-metal Spartan Plus specimens, the main reason for this sharp decrease in fatigue resistance for the all-old metal specimens is probably from the loss of secondary elements during remelting. Therefore, when casting high-palladium alloys, the standard dental laboratory practice [19] of using at least 50% new metal should be followed in order to obtain optimum fatigue properties.

5. Conclusions

Under the conditions of this study, the following conclusions can be drawn:

1. Using cyclic tension-compression loading with a stress amplitude ratio of $R = -1$, the fatigue limits (2×10^6 cycles) for all-new metal specimens of the Pd-Cu-Ga alloy Spartan Plus and the Pd-Ga alloy Protocol were approximately 0.20 and 0.15 of the 0.1% yield strength (YS) in tension for each alloy, respectively. Specimens were in the clinically relevant heat-treated condition that simulated the porcelain firing cycles.

2. The fatigue-resistance of Spartan Plus and Protocol specimens containing 50% old metal (previously melted one time) and 50% new metal after simulated porcelain-firing heat treatment is comparable to that of specimens containing all-new metal.

3. The fatigue resistance of heat-treated Spartan Plus specimens, where all of the metal was previously melted one time, decreases dramatically. In order to maintain adequate fatigue resistance, at least 50% new metal should be used when remelting scrap metal of Spartan Plus that was previously melted one time.

4. The fatigue properties of Spartan Plus specimens after simulated porcelain-firing heat treatment were not adversely affected by remnants of the original as-cast dendritic microstructure in the relatively large test specimens. A longer heat treatment is evidently needed to completely eliminate the as-cast dendritic structure in specimens of this size.

5. Spartan Plus exhibits superior fatigue resistance to Protocol, which has an equiaxed-grain microstructure. This is consistent with the greater tensile yield strength of Spartan Plus that was previously found using the same specimen dimensions as for the fatigue testing.

Acknowledgments

This research was supported by Grant DE10147 from the National Institute of Dental and Craniofacial Research of the National Institutes of Health, Bethesda, MD, USA. We want to thank Andrew Stevenson in the College

Fixed Prosthodontics Laboratory for his expert technical assistance in preparing the castings, Lloyd Barnhart in the Department of Materials Science and Engineering for expert technical assistance with the fatigue testing, and Dr. Wayne Wozniak of the American Dental Association for providing the plastic patterns used for casting the test specimens.

References

1. A. B. CARR and W. A. BRANTLEY, *Int. J. Prosthodont.* **4** (1991) 265.
2. R. B. STEWART, K. GRETZ and W. A. BRANTLEY, *J. Dent. Res.* **71** (1992) 158, Abstract No. 423.
3. E. PAPAOGLOU, Q. WU, W. A. BRANTLEY, J. C. MITCHELL and G. MEYRICK, *Cells Mater.* **9** (1999) 43.
4. E. PAPAOGLOU, Q. WU, W. A. BRANTLEY, J. C. MITCHELL and G. MEYRICK, *J. Mater. Sci.: Mater. Med.* **11** (2000) 601.
5. E. PAPAOGLOU, W. A. BRANTLEY, A. B. CARR and W. M. JOHNSTON, *J. Prosthet. Dent.* **70** (1993) 386.
6. E. PAPAOGLOU and W. A. BRANTLEY, *Dent. Mater.* **14** (1998) 112.
7. E. PAPAOGLOU, W. A. BRANTLEY, W. M. JOHNSTON and A. B. CARR, *J. Prosthet. Dent.* **79** (1998) 514.
8. M. M. STAVRIDAKIS, E. PAPAOGLOU, R. R. SEGHI, W. M. JOHNSTON and W. A. BRANTLEY, *J. Prosthodont.* **9** (2000) 71.
9. M. C. NUTT, in "Metallurgy and Plastics for Engineers" (Pergamon Press, Oxford, UK, 1976), p. 360.
10. H. W. ANSELM WISKOTT, J. I. NICHOLLS and U. C. BELSER, *Int. J. Prosthodont.* **8** (1995) 105.
11. G. E. DIETER, in "Mechanical Metallurgy", 3rd edn (McGraw-Hill, New York, 1986), Chap 9.
12. N. E. DOWLING, in "Mechanical Behavior of Materials: Engineering Methods for Deformation, Fracture and Fatigue" (Prentice Hall, Englewood Cliffs, NJ, USA, 1993), Chaps 9–11.
13. B. S. KELLY, W. A. BRANTLEY, J. A. HOLLOWAY, A. S. LITSKY, J. C. MITCHELL and D. LI, *J. Dent. Res.* **79** (2000) 188, Abstract No. 355.
14. W. A. BRANTLEY, Z. CAI, D. W. FOREMAN, J. C. MITCHELL, E. PAPAOGLOU and A. B. CARR, *Dent. Mater.* **11** (1995) 154.
15. W. A. BRANTLEY, Z. CAI, A. B. CARR and J. C. MITCHELL, *Cells Mater.* **3** (1993) 103.
16. ANSI/ADA Specification No. 5 for dental casting alloys (Council on Dental Materials, Instruments and Equipment, Chicago, IL, USA, 1988).
17. ANSI/ADA Specification No. 38 for metal-ceramic systems (Council on Dental Materials, Instruments and Equipment, Chicago, IL, USA, 1991).
18. D. A. BRIDGEPORT, W. A. BRANTLEY and P. F. HERMAN, *J. Prosthodont.* **2** (1993) 144.
19. R. G. CRAIG (ed), "Restorative Dental Materials", 10th edn (Mosby, St. Louis, 1997), pp. 456 and 496.
20. W. A. BRANTLEY, Q. WU, Z. CAI, S. G. VERMILYEA, J. C. MITCHELL and M. C. COMERFORD, *Cells Mater.* **9** (1999) 83.
21. K. J. ANUSAVICE, in "Phillips' Science of Dental Materials", 10th edn (Saunders, Philadelphia, 1996), pp. 517–522.
22. H. JIANG, P. BOWEN and J. F. KNOOT, *J. Mater. Sci.* **34** (1999) 719.
23. A. A. DABAYEH, R. X. XU, B. P. DU and T. H. TOPPER, *Int. J. Fatig.* **18** (1996) 95.
24. P. HEULER, C. BERGER and J. MOTZ, *Fatig. Fract. Eng. Mater. Struct.* **16** (1993) 115.
25. W. GUO, W. A. BRANTLEY, W. A. T. CLARK, D. LI and P. MONAGHAN, *J. Mater. Sci.: Mater. Med.* **13**(4) 369–374.

Received 14 June
and accepted 7 September 2001